Studies of the collision-based Xe VI and Xe VII spectra

M. Wang, A. Arnesen, R. Hallin, F. Heijkenskjöld, M. O. Larsson,* and A. Wännström

Department of Physics, Uppsala University, Box 530, S-75121 Uppsala, Sweden

A. G. Trigueiros

Instituto de Física "Gleb Wataghin," Universidade Estadual de Campinas, 13083-970 Campinas, São Paulo, Brasil

A. V. Loginov

Vavilov State Optical Institute, St. Petersburg 199034, Russia

Received April 21, 1997; revised manuscript received July 14, 1997

Collision-based spectroscopy of a Xe^{q+} ($q = 6, 7$) beam with a target T (T = Na, Ar) has been performed in the 35–800-nm wavelength region. Twenty-five new Xe VI lines and twenty-two new Xe VII lines were classified, twelve new energy levels of Xe VI and nine new energy levels of Xe VII were established, and one energy level of Xe VI was revised from the classified transitions. The analysis was supported by Hartree–Fock calculations. © 1997 Optical Society of America [S0740-3224(97)00512-2]

1. INTRODUCTION

The spectrum of five-times-ionized xenon, Xe VI, is in the In isoelectronic sequence with a ground configuration of $5s^25p$. The early reports on Xe VI were made by Fawcett and Bromage,[1] who used a toroidal zeta device, and by Kernahan *et al.*,[2] who used beam-foil spectroscopy. Subsequently Kaufman and Sugar[3] completed the energy levels of the $5s^25p$, $5s^25d$, and $5s^26s$ configurations and the doublet levels of the $5s5p^2$ configuration. Tauheed *et al.*[4] completed the $5s5p^2$ configuration by adding the three $5s5p^2\ ^4P$ levels. A trigged spark was used as a light source. Recently Larsson *et al.*[5] reported the $5s^26p\ ^2P_{3/2}$ and two doublet $5s^24f\ ^2F$ levels, and Wang *et al.*[6] extended the levels to Rydberg states and gave the ionization limit, using collision-based spectroscopy.

The spectrum of six-times-ionized xenon, Xe VII, is Cd-like, with a ground configuration of $5s^2$. It was previously investigated by a number of groups of researchers[7–13] who used various methods such as beam-foil spectroscopy, spark-light sources, laser produced plasmas, theta pinches, etc. The details of several investigations were recently given by Cavalcanti *et al.*[13] The energy levels of $5s^2$, $5s5p$, $5p^2$, $5s5d$, $5s6s$, and $5p5d$ configurations as well as the ionization limit were determined. In a recent investigation, Larsson *et al.*[14] obtained energy levels of the $5s6s$, $5s5d$, $5p^2$, and $5s4f$ configurations by collision-based spectroscopy.

In this paper we report on the additional observations and analysis of Xe VI and Xe VII. This study is a continuation of our investigations of multiply charged xenon ions in which we used collision-based spectroscopy for charge-state discrimination and level-population selectivity.[5,6] We classified 25 lines in the Xe VI spectrum and completed the $5s^27s$, $5s^28s$, $5s^26p$, $5s^27p$, $5s^28p$, $5s^26d$, $5s^27d$, and $5s^28d$ configurations based on these transitions. We also established the energy levels of some Xe VII configurations: two $5s6p\ ^3P_{0,2}$ levels, three $5s6d\ ^3D$ triplet levels, three $5s7p\ ^3P$ triplet levels, and the $5s7s\ ^3S_1$ level based on new transitions observed in the Xe VII spectrum. Using a least-squares approach, we interpreted the energy-level assignments of Xe VII by fitting the energy levels in the Cd I isoelectronic sequence.

2. EXPERIMENT

The details of our experimental system for collision-based spectroscopy of multiply charged ions were described in a previous paper.[15] Multiply charged xenon ions were produced in an electron cyclotron resonance ion source at a potential of 10 kV. Xe^{6+} and Xe^{7+} beams were formed by q/m analysis in a 90° double-focusing dipole magnet. The beams were then focused onto the target cell by an electrostatic Einzel lens. Typical ion currents, measured with a Faraday cup situated downstream from the cell, were ~2 μA. The target was either a differentially pumped gas cell filled with Ar gas or an effusive Na beam from an oven with the outlet heated to ~600 K. The pressure inside the gas cell was kept high enough to give a reasonable count rate but low enough to limit the probability of multiple collisions before the projectile ion reached the observation region. The collision-induced photon emission from the ion–atom interaction zone was observed in the wavelength region 35–800 nm perpendicularly to the ion-beam direction by a 1-m normal-incidence spectrometer with 1200/mm grooves. In the UV–visible wavelength region we used a Jobin-Yvon Hr 1000 Czerny–Turner-type monochromator with a photomultiplier tube as the detector, whereas an evacuated

0740-3224/97/123277-05$10.00

Table 1. Observed Xe VI Lines Classified in This Work

λ_{obs} (nm)[a]	λ_{HFR} (nm)[b]	I_{Na}[c]	I_{Ar}[c]	gA ($\times 10^9$)[d]	Transition	Δ (cm^{-1})[e]
60.78	57.51	148	287	0.1	$5s5p^2\ ^4P_{3/2}$–$5s^26p\ ^2P_{1/2}$	18
65.93	65.66	312	184	138.00	$5s^25d\ ^2D_{3/2}$–$5s^25f\ ^2F_{5/2}$	−3
66.96	66.63	515	228	188.30	$5s^25d\ ^2D_{5/2}$–$5s^25f\ ^2F_{7/2}$	−1
67.17	67.71	41	–	1.07	$5s^26p\ ^2P_{1/2}$–$5s^28s\ ^2S_{1/2}$	60
69.78	69.56	161	–	1.67	$5s^26p\ ^2P_{3/2}$–$5s^28s\ ^2S_{1/2}$	−93
71.42	68.64	360	993	1.42	$5s5p^2\ ^2D_{3/2}$–$5s^26p\ ^2P_{1/2}$	−1
118.14[f]	122.40	764		2.59	$5s^25d\ ^2D_{3/2}$–$5s^26p\ ^2P_{1/2}$	7
122.04	121.86	184		3.23	$5s^26p\ ^2P_{3/2}$–$5s^27s\ ^2S_{1/2}$	0
135.98	135.38	113	–	6.30	$5s^26p\ ^2P_{1/2}$–$5s^26d\ ^2D_{3/2}$	−16
143.92	140.84	236	–	8.05	$5s^26p\ ^2P_{3/2}$–$5s^26d\ ^2D_{5/2}$	14
145.98	145.20	79	–	0.066	$5s^27p\ ^2P_{1/2}$–$5s^28d\ ^2D_{3/2}$	−89
147.74	147.54	141	–	0.19	$5s^27p\ ^2P_{3/2}$–$5s^28d\ ^2D_{5/2}$	41
241.49	259.80	109	196	0.73	$5s^26s\ ^2S_{1/2}$–$5s^26p\ ^2P_{1/2}$	−1
253.14	258.45	1310	–	0.53	$5s^27p\ ^2P_{1/2}$–$5s^28s\ ^2S_{1/2}$	−23
261.70	267.62	2479	–	1.02	$5s^27p\ ^2P_{3/2}$–$5s^28s\ ^2S_{1/2}$	8
279.89	284.61	1521	–	0.47	$5s^26d\ ^2D_{3/2}$–$5s^27p\ ^2P_{1/2}$	−5
	282.60			0.97	$5s^26d\ ^2D_{5/2}$–$5s^27p\ ^2P_{3/2}$	0
334.19	334.43	639	–	1.56	$5s^27p\ ^2P_{1/2}$–$5s^27d\ ^2D_{3/2}$	0
339.83	345.41	668	–	2.81	$5s^27p\ ^2P_{3/2}$–$5s^27d\ ^2D_{5/2}$	0
430.08	411.09	253	–	0.87	$5s^27s\ ^2S_{1/2}$–$5s^27p\ ^2P_{3/2}$	−6
455.86	434.79	100	–	0.32	$5s^27s\ ^2S_{1/2}$–$5s^27p\ ^2P_{1/2}$	3
512.84	527.48	123	–	1.05	$5s^28p\ ^2P_{1/2}$–$5s^28d\ ^2D_{3/2}$	0
518.06[f]	469.53	270	–	0.10	$5s^27d\ ^2D_{5/2}$–$5s^28p\ ^2P_{3/2}$	0
521.65	499.76	67	–	0.49	$5s^27d\ ^2D_{3/2}$–$5s^28p\ ^2P_{1/2}$	−1
528.67	558.57	172	–	1.39	$5s^28p\ ^2P_{3/2}$–$5s^28d\ ^2D_{5/2}$	−1

[a] Observed vacuum wavelengths.
[b] HFR-calculated vacuum wavelengths.
[c] Intensity of lines observed following Xe^{6+} collisions with Na or Ar. A dash means that the line was not visible in the spetrum.
[d] HFR-calculated gA values.
[e] $\Delta = \sigma_{obs} - \sigma_{levels}$, where σ_{levels} is the transition energy obtained from levels given in Refs. 3–6 and new levels given in Table 2.
[f] Blend.

spectrometer with either a channeltron or a solar-blind photomultiplier tube was used in the vacuum-ultraviolet wavelength region.

Photon emission spectra of Xe^{q+}–Na ($q = 6, 7$) collisions in the 35–800-nm wavelength region and of Xe^{q+}–Ar ($q = 6, 7$) collisions in the 35–120- and 200–800 nm wavelength regions were recorded. We calibrated the wavelength scale by fitting the coefficients of a polynomial, expressing the wavelength as a function of line position, to the wavelengths and line positions of known Xe VI and Xe VII lines. The uncertainty of the wavelengths obtained in this way varies with line intensity and wavelength region. For lines of typical intensity, the uncertainties are estimated to be 0.04, 0.06, and 0.08 nm for the regions 35–120, 120–240, and 200–800 nm, respectively.

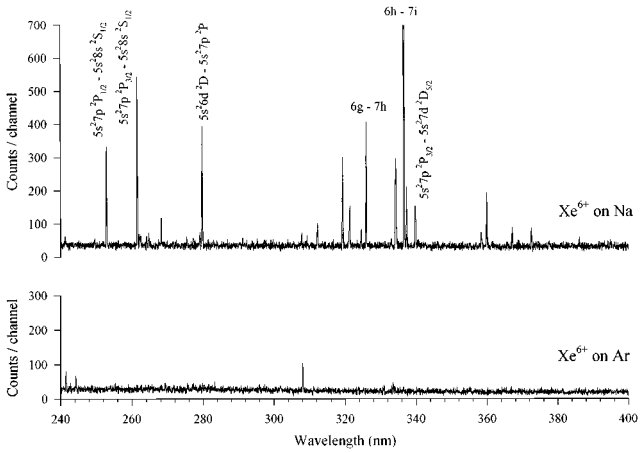

Fig. 1. Spectra of Xe^{6+}–Na and Xe^{6+}–Ar collisions in the 240–400-nm wavelength region.

3. RESULTS AND DISCUSSION

The identification of the spectral lines was based on Hartree–Fock calculations[16] and level populations predicted by the classical over-the-barrier model.[17] We also used previously recorded $Xe^{6+,7+}$–He spectra in the region 35–800 nm and $Xe^{6+,7+}$–Ar spectra in the region 120–250 nm (Refs. 5 and 14) in our data analysis. The Xe^{q+}–Ar ($q = 6, 7$) spectra in the 35–120 and 200–800-nm wavelength regions completed the Xe^{q+}–Ar ($q = 6, 7$) spectrum in the region 35–800 nm. Therefore we comprehensively compared the three different target spectra in the 35–800-nm region.

A. Xe VI

The study of Xe VI is an extension of a previous one of the wavelengths and energy levels of Rydberg states of Xe VI

published by Wang *et al.*[6] Classifications, wavelengths, and intensities (not calibrated) of the identified lines of Xe VI as well as the wavelengths calculated by the Hartree–Fock method with relativistic corrections are given in Table 1.

Energy levels for $n \leqslant 8$ configurations as well as transition wavelengths and probabilities were calculated by Cowan's HFR code, and the radial electrostatic integrals were scaled to 85%. The radial spin–orbit integrals were not adjusted. Because of the overlap among the $5s^26d$ and $5s5p4f$, $5s^27p$ and $5s5p6s$, and $5s^28p$ and $5s5p6d$ configurations, the configuration interaction is quite large and significantly influences the energy-level structure. Therefore we included in our calculation the even-parity configurations $5s5p^2$, $5s5p4f$, and $5s5d^2$ and the odd-parity configurations $5s5p5d$, $5s5p6s$, and $5s5p6d$.

The level energies of the most populated singly excited Xe^{5+} states were predicted by the classical over-the-

Table 2. Energy Levels of Xe VI (cm^{-1}) Established in This Work

Level	E_{exp} (cm^{-1})[a]	$E_{exp} - E_{HFR}$[b]	Percent Composition[c]
$5s^27s\ ^2S_{1/2}$	352 250 ± 43	965	100
$5s^28s\ ^2S_{1/2}$	413 710 ± 44	733	100
$5s^26p\ ^2P_{1/2}$	264 890 ± 15[d]	−390	97
$5s^27p\ ^2P_{1/2}$	374 180 ± 43	−105	69% $5s^27p\ ^2P_{1/2}$ + 29% $5p6s\ ^2P_{1/2}$
$5s^27p\ ^2P_{3/2}$	375 500 ± 43	−106	78% $5s^27p\ ^2P_{3/2}$ + 21% $5p6s\ ^2P_{3/2}$
$5s^28p\ ^2P_{1/2}$	423 270 ± 44	−921	99
$5s^28p\ ^2P_{3/2}$	424 230 ± 44	−1246	86% $5s^28p\ ^2P_{3/2}$ + 8% $5p6d\ ^2P_{3/2}$
$5s^26d\ ^2D_{3/2}$	338 450 ± 34	−699	55% $5s^26d\ ^2D_{3/2}$ + 43% $5p4f\ ^2D_{3/2}$
$5s^26d\ ^2D_{5/2}$	339 770 ± 34	−450	54% $5s^26d\ ^2D_{5/2}$ + 44% $5p4f\ ^2D_{5/2}$
$5s^27d\ ^2D_{3/2}$	404 100 ± 44	−81	100
$5s^27d\ ^2D_{5/2}$	404 930 ± 44	346	100
$5s^28d\ ^2D_{3/2}$	442 770 ± 45	−379	99
$5s^28d\ ^2D_{5/2}$	443 150 ± 45	−237	99

[a] The experimental energies are based on levels given in Refs. 3–6 and wavelengths of Table 1.
[b] HFR calculations.
[c] HFR calculations. Only percentages larger than 3 are listed.
[d] Revision of energy given in Ref. 6.

Table 3. Observed Xe VII Lines Classified in This Work

λ_{obs} (nm)[a]	λ_{HFR} (nm)[b]	I_{Na}[c]	I_{Ar}[c]	gA ($\times 10^9$)[d]	Transition	Δ (cm^{-1})[e]
57.69[f]	57.63	299	1181	0.15	$5p^2\ ^3P_1$–$5s6p\ ^3P_2$	−56
58.17	58.19	310	1662	4.93	$5p^2\ ^1D_2$–$5s6p\ ^3P_2$	−69
83.73	84.55	69	–	1.48	$5s5d\ ^3D_2$–$5s6p\ ^3P_2$	65
84.94	85.48	851	1601	14.43	$5s5d\ ^3D_3$–$5s6p\ ^3P_2$	−10
88.41	89.43	193	431	1.64	$5s5d\ ^3D_1$–$5s6p\ ^3P_1$	27
88.70	89.76	528	917	2.64	$5s5d\ ^3D_1$–$5s6p\ ^3P_0$	9
89.16	90.08	356	739	4.18	$5s5d\ ^3D_2$–$5s6p\ ^3P_1$	16
94.93	94.88	–	56	3.97	$5s6p\ ^3P_1$–$5s7s\ ^3S_1$	−39
100.04	99.80	42	154	2.30	$5s5d\ ^3D_2$–$5p5d\ ^3F_2$	−65
101.87	102.12	–	154	6.30	$5s6p\ ^3P_2$–$5s7s\ ^3S_1$	9
109.44	116.28	38	–	0.38	$5s5p\ ^1P_1$–$5p^2\ ^3P_1$	−47
132.48	132.43	1291	154	6.31	$5s6p\ ^3P_0$–$5s6d\ ^3D_1$	0
132.71	132.58	779	74	12.13	$5s6p\ ^3P_1$–$5s6d\ ^3D_2$	−12
145.48	145.39	1028	141	17.81	$5s6p\ ^3P_2$–$5s6d\ ^3D_3$	14
187.76	192.09	484	25	4.27	$5s6s\ ^3S_1$–$5s6p\ ^3P_2$	13
190.23	190.43	217	–	5.58	$5s6d\ ^3D_3$–$5s7p\ ^3P_2$	28
194.96	195.47	171	–	2.63	$5s6d\ ^3D_2$–$5s7p\ ^3P_1$	8
195.76	195.63	138	–	1.23	$5s6d\ ^3D_1$–$5s7p\ ^3P_0$	0
196.73	194.91	279	–	0.61	$5p5d\ ^3P_1$–$5s6d\ ^3D_2$	12
219.02	225.31	124	119	0.60	$5s6s\ ^3S_1$–$5s6p\ ^3P_0$	−12
432.90	431.77	237	–	1.07	$5s7s\ ^3S_1$–$5s7p\ ^3P_2$	−9
470.33	471.94	86	–	0.43	$5s7s\ ^3S_1$–$5s7p\ ^3P_1$	−7

[a] Observed vacuum wavelengths.
[b] HFR-calculated vacuum wavelengths.
[c] Intensity of lines observed following Xe^{7+} collisions with Na or Ar. A dash means that the line was not visible in the spectrum.
[d] HFR-calculated gA values.
[e] $\Delta = \sigma_{obs} - \sigma_{levels}$, where σ_{levels} is the transition energy obtained from levels given in Refs. 7–14 and new levels given in Table 4.
[f] Blend.

Table 4. Energy Levels of Xe VII (cm^{-1}) Established in This Work

Level	$E_{exp}(cm^{-1})$[a]	$E_{exp} - E_{calc}$[b]	Percent Composition[c]
$5s6p\ ^3P_0$	400 500 ± 19	−42	97
$5s6p\ ^3P_1$	400 854[d]	42	82% $5s6p\ ^3P_1$ + 14% $5s6p\ ^1P_1$ + 3% $5p5d\ ^3P_1$
$5s6p\ ^3P_2$	408 080 ± 19	17	84% $5s6p\ ^3P_2$ + 13% $5p5d\ ^3F_2$
$5s6d\ ^3D_1$	475 990 ± 40	24	100
$5s6d\ ^3D_2$	476 220 ± 40	−35	99
$5s6d\ ^3D_3$	476 800 ± 40	11	100
$5s7p\ ^3P_0$	527 070 ± 45	−66	100
$5s7p\ ^3P_1$	527 500 ± 45	69	86% $5s7p\ ^3P_1$ + 14% $5s7p\ ^1P_1$
$5s7p\ ^3P_2$	529 340 ± 45	14	99
$5s7s\ ^3S_1$	506 230 ± 48	0	100

[a] The experimental energies are based on levels given in Refs. 7–14 and wavelengths of Table 3.
[b] Energy levels obtained from the least-squares fitting calculations.
[c] HFR calculations. Only percentages larger than 3 are listed. Underlined numbers indicate negative eigenvectors.
[d] Energy level from Ref. 12.

barrier model. The levels above $5s^26p$ could be populated only by the Na target (Fig. 1), as discussed in Ref. 6. Consequently for these highly excited levels it is impossible to compare the intensity ratios among different targets for transition assignments. Thus the identifications of the transitions from these levels relied mainly on the agreement between calculated and observed branching ratios.

In the Xe^{6+}–Na spectra we identified the two lines at 114.69 and 122.04 nm as the $5s^26p\ ^2P$–$5s^27s\ ^2S$ transitions. These two lines appeared also in the Xe^{6+}–He spectra recorded by Larsson *et al.*,[5] which should not be possible according to the classical over-the-barrier model. The intensity ratios are the same with He and Na targets. Possibly the $5s^27s\ ^2S$ state was generated by means of single-electron capture from He onto metastable Xe^{6+} ions, which, to some extent, were present in the ion beam.

The establishment of energy levels was based on known energy levels as well as on the observation of the transitions given in Table 1. Energy levels established in this work are listed in Table 2. The level energy of $5s^26p\ ^2P_{1/2}$ was erroneously given as 264 137 cm^{-1} by Wang *et al.*,[6] who identified a line at 119.21 nm as $5s^25d\ ^2D_{3/2}$–$5s^26p\ ^2P_{1/2}$. In the Xe^{6+}–Ar and the Xe^{6+}–Na spectra we recorded lines at 118.14 and 241.49 nm. We identified these two lines as the $5s^25d\ ^2D_{3/2}$–$5s^26p\ ^2P_{1/2}$ and the $5s^26s\ ^2S_{1/2}$–$5s^26p^2P_{1/2}$ transitions, respectively. The revised level energy of $5s^26p\ ^2P_{1/2}$ is generated from these two transitions. The two other $5s5p^2$–$5s^26p\ ^2P_{1/2}$ transitions at 60.78 and 71.42 nm support this level assignment. Also, the intensities of the transitions originating from the $5s^26p\ ^2P_{1/2}$ level are relatively stronger in the Ar spectra than in the Na spectra, in agreement with the classical over-the-barrier model prediction.

B. Xe VII

We included 20 configurations in the HFR calculation of Xe VII. As for Xe VI, we scaled the radial electrostatic integrals to 85%, but the radial spin–orbit integrals were kept to 100%. The classified wavelengths and intensities of all the identified lines and the HFR calculated wavelengths are given in Table 3. The $5s6p\ ^3P_2$ level energy

Table 5. Least-Squares-Fitted Radial Integrals and Configuration Average Energies (in cm^{-1}) for the $5s6p$, $5s6d$, $5s7p$ Configurations of Xe VII[a]

Configuration	Parameter	LSF Value	HFR Value	LSF/HFR
$5s6p$	E_{av}	405 775(34)	394 325	1.030
	$G^1(5s6p)$	1 313(176)	6 907	0.190
	ζ_{6p}	5 014(46)	3 534	1.419
$5s6d$	E_{av}	477 428(23)	464 775	1.027
	$G^1(5s6d)$	9 685(135)	7 776	1.245
	ζ_{6d}	330(24)	376	0.878
$5s7p$	E_{av}	529 282(52)	516 739	1.024
	$G^1(5s7p)$	1 738(248)	2 545	0.683
	ζ_{7p}	1 856(75)	1 779	1.043

[a] Configuration interaction parameters were fixed as HFR values.

Table 6. Least-Squares-Fitted Radial Integrals and Configuration Average Energies (in cm^{-1}) for the $5s6p$ Configurations in the Cd I Isoelectronic Sequence

Title	Parameter	LSF Value	HFR Value	LSF/HFR
Cd I	E_{av}	58 897(1)	51 084	1.153
	$G^1(5s6p)$	2 014(2)	2 863	0.703
	ζ_{6p}	164(1)	138	1.188
In II	E_{av}	108 552(3)	99 826	1.087
	$G^1(5s6p)$	2 304(10)	4 082	0.564
	ζ_{6p}	513(4)	430	1.193
Sn III	E_{av}	161 330(2)	152 009	1.061
	$G^1(5s6p)$	2 352(10)	4 838	0.486
	ζ_{6p}	1 001(4)	834	1.200
Sb IV	E_{av}	217 391(1)	207 607	1.047
	$G^1(5s6p)$	2 362(3)	5 428	0.435
	ζ_{6p}	1 610(1)	1 341	1.200
Te V	E_{av}	276 738(6)	266 554	1.038
	$G^1(5s6p)$	2 391(29)	5 959	0.401
	ζ_{6p}	2 334(9)	1 959	1.191
Xe VII	E_{av}	405 775(34)	394 325	1.030
	$G^1(5s6p)$	1 313(176)	6 907	0.190
	ζ_{6p}	5 014(46)	3 534	1.419

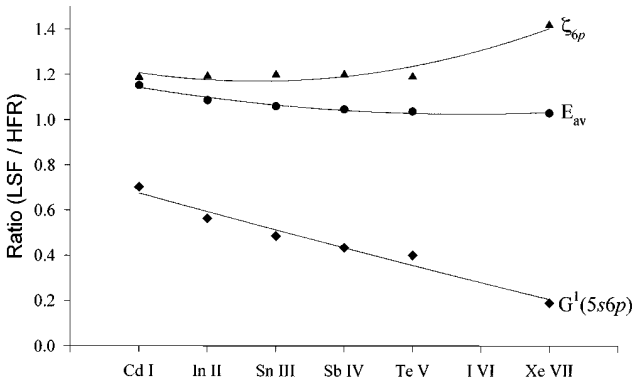

Fig. 2. Ratios between least-squares-fitted and HFR calculated parameter values of the $5s6p$ configuration in the Cd I sequence. ζ_{6p}, E_{av}, and $G^1(5s6p)$ have been plotted.

is obtained from the transitions $5s5d\ ^3D_3$–$5s6p\ ^3P_2$ and $5s6s\ ^3S_1$–$5s6p\ ^3P_2$ at 84.94 and 187.76 nm, respectively. The $5s6p\ ^3P_0$ level is obtained from $5s5d\ ^3D_1$–$5s6p\ ^3P_0$ and $5s6s\ ^3S_1$–$5s6p\ ^3P_0$ at 88.70 and 219.02 nm, respectively. The establishment of the three $5s6d\ ^3D$ levels, the three $5s7p\ ^3P$ levels, and the $5s7s\ ^3S_1$ level is based on the three triplet $5s6p$ levels. The levels established in this study are listed in Table 4.

We made a least-squares fitting (LSF) of the radial integrals to the derived levels for further confirmation of the classifications. The results of the LSF calculations are given in Table 5, including the old configurations $5s6p$ and $5s7p$ and the even configuration $5s6d$. The fitted values of $G^1(5s6p)$ and ζ_{6p} in Table 5 have a large variance with the HFR calculated values. Therefore we also made a LSF for the $5s6p$ configuration in the Cd I isoelectronic sequence. The $5s6p$ energy levels of Cd I–Te V are from Refs. 18 and 19. The fitted parameter values are listed in Table 6, and the ratios between LSF values and HFR values are plotted in Fig. 2.

4. CONCLUSION

In summary, we have investigated the photon emission from excited Xe^{5+} and Xe^{6+} ions in the wavelength range from vacuum ultraviolet to visible light following electron capture by Xe^{6+} and Xe^{7+} beams in collisions with Na or Ar. In total, we have classified 47 new transitions and established 22 new energy levels of Xe VI and Xe VII. The line identifications were supported by Hartree–Fock calculations. The Na target used in this study has proved useful in establishing highly excited states of multiply charged ions.

ACKNOWLEDGMENT

This research was supported by The Swedish Natural Science Research Council. We thank T. Chen for programming support.

*Present address, Institute of Physics and Astronomy, University of Aarhus, DK-8000 Aarhus C, Denmark.

REFERENCES

1. B. C. Fawcett and G. E. Bromage, "Classification of krypton VI, V and xenon VI spectral lines," J. Phys. B **13**, 2711–2716 (1980).
2. J. A. Kernahan, E. H. Pinnington, J. A. O'Neill, J. L. Bahr, and K. E. Donnelly, "Study of the beam-foil spectrum of Xe VI, Xe VII, and Xe VIII from 500 to 1550 Å," J. Opt. Soc. Am. **70**, 1126–1129 (1980).
3. V. Kaufman and J. Sugar, "In I isoelectronic sequence: wavelengths and energy levels for Xe VI through La IX," J. Opt. Soc. Am. B **4**, 1924–1926 (1987).
4. A. Tauheed, Y. N. Joshi, and E. H. Pinnington, "The $5s^25p\ ^2P$–$5s5p^2\ ^4P$ intercombination lines in the In I isoelectronic sequence from Sb III to La IX," J. Phys. B **25**, L561–L564 (1992).
5. M. O. Larsson, A. M. Gonzalez, R. Hallin, F. Heijkenskjöld, B. Nyström, G. O'Sullivan, C. Weber, and A. Wännström, "Wavelengths and energy levels of Xe V and Xe VI obtained by collision-based spectroscopy," Phys. Scr. **53**, 317–324 (1996).
6. M. Wang, M. O. Larsson, A. Arnesen, R. Hallin, F. Heijkenskjöld, C. Nordling, and A. Wännström, "Collision-based spectroscopy of Xe VI Rydberg states," J. Opt. Soc. Am. B **13**, 2715–2719 (1996).
7. B. C. Fawcett, B. B. Jones, and R. Wilson, "Vacuum ultraviolet spectra of multiply ionized inert gases," Proc. Phys. Soc. London **78**, 1223–1226 (1961).
8. E. J. Knystautas, J. Sugar, and J. R. Roberts, "New line classifications and energy levels in the triplet system of Xe VII," J. Opt. Soc. Am. **69**, 1726–1727 (1979).
9. R. Hallin, J. A. Leavitt, A. Lindgård, P. W. Rathmann, H. Vach, and E. Veje, "Beam-foil excitation of xenon, 4 MeV," Nucl. Instrum. Methods **202**, 41–44 (1982).
10. G. O'Sullivan, "Charge-dependent wavefunction collapse in ionised xenon," J. Phys. B **15**, L765–L771 (1982).
11. J. Blackburn, P. K. Carroll, J. Costello, and G. O'Sullivan, "Spectra of Xe VII, VIII, and IX in the extreme-ultraviolet $4d$-mp, nf transitions," J. Opt. Soc. Am. **73**, 1325–1329 (1983).
12. V. Kaufman and S. Sugar, "Cd I isoelectronic sequence: wavelengths and energy levels for Xe VII through Eu XVI," J. Opt. Soc. Am. B **4**, 1919–1923 (1987).
13. G. H. Cavalcanti, F. R. T. Luna, A. G. Trigueiros, F. Bredice, H. Sobral, R. Hutton, and M. Wang, "The vacuum-ultraviolet spectrum of six times ionized xenon, Xe VII," J. Opt. Soc. Am. B **14**, 2459 (1997).
14. M. O. Larsson, A. M. Gonzalez, R. Hallin, F. Heijkenskjöld, R. Hutton, A. Langereis, B. Nyström, G. O'Sullivan, and A. Wännström, "Wavelengths and energy levels of Xe VII and Xe VIII obtained by collision-based spectroscopy," Phys. Scr. **51**, 69–75 (1995).
15. M. Wang, A. Arnesen, R. Hallin, F. Heijkenskjöld, A. Langereis, M. O. Larsson, C. Nordling, and A. Wännström, "Collision-based spectroscopy of Xe VIII Rydberg states," J. Opt. Soc. Am. B **13**, 1650–1658 (1996).
16. R. D. Cowan, *The Theory of Atomic Structure and Spectra* (U. California Press, Berkeley, Calif., 1981).
17. A. Bárány, "Barrier models describing collisions of highly charged ions," Phys. Scr. **42**, 280–284 (1990).
18. C. E. Moore, "Atomic energy levels," Natl. Bur. Stand. (U.S.) Circ. **467** (1958), Vol. III, pp. 55–102.
19. A. M. Crooker and Y. N. Joshi, "Spark spectra of tellurium," J. Opt. Soc. Am. **54**, 553–554 (1964).